JACS
JOURNAL OF THE AMERICAN CHEMICAL SOCIETY

Communication

pubs.acs.org/JACS

Mapping the Details of Contact Effect of Modulated Au-Octanedithiol-Au Break Junction by Force–Conductance Cross-Correlation

Kun Wang, Joseph M. Hamill, Jianfeng Zhou, and Bingqian Xu*

Single Molecule Study Laboratory, College of Engineering and Nanoscale Science and Engineering Center, University of Georgia, Athens, Georgia 30602, United States

Supporting Information

ABSTRACT: We have measured the force and conductance of Au-octanedithiol-Au junctions using a modified conducting atomic force microscopy break junction technique with sawtooth modulations. Force–conductance two-dimensional cross-correlation histogram (FC-2DCCH) analysis for the single-molecule plateaus is demonstrated. Interestingly, four strong correlated regions appear in FC-2DCCHs consistently when modulations with different amplitudes are applied, in sharp contrast to the results under no modulation. These regions reflect the conductance and force changes during the transition of two molecule/electrode contact configurations. As the modulation amplitude increases, intermediate transition states of the contact configurations are discerned and further confirmed by comparing individual traces. This study unravels the relation between force and conductance hidden in the data of a modulated single-molecule break junction system and provides a fresh understanding of electron transport properties at molecule/electrode interfaces.

The single-molecule break junction (SMBJ) technique has been performed as a reliable experimental platform, creating electrode-molecule-electrode structures.[1−6] Studies using SMBJ focus on the charge transport properties, namely, the conductance, of molecular junctions.[6−9] Precise control of the atomic structure, however, is not well achieved. Large fluctuations in the conductance measurements of alkane molecules have been puzzling and are not yet fully understood.[5,10] For instance, a Au-octanedithiol (C8DT)-Au junction was measured to have >1 order difference in conductance.[11−14] Such uncertainty in conductance has also been observed for other molecules in the alkane family.[11,12,14] Theoretical simulations proposed the variation at the molecule/electrode contact interfaces as the cause for the broad distribution in conductance.[4,12,15−17] Equally important is that a series of changes in contact configurations along the evolution of a single-molecule junction prior to rupture could also induce significant conductance change, especially for Au-thiol (Au-S) contact.[18−20] Thus, to incorporate science derived from a SMBJ, a better understanding of the molecule/electrode interfaces is key.

Sawtooth modulation of piezotransducer (PZT) movement on a stabilized molecular junction has been proven to be able to isolate the contact parts for detailed study, and individual traces measured under such modulation show a close kinship between force and conductance.[21,22] However, conventional 1D and 2D histograms are not ideal tools to discover significant information from these modulated traces, and the lack of a proper method to interpret the modulated data hinders the physical understanding of contact effect.[21] Recent applications of correlation analysis on conductance traces showed more detailed features beyond conventional histograms and provided a new understanding of molecular junctions.[23−25] A more recent promotion of the correlation analysis involved a multivariate time series analysis by adding a second, variable force to the analysis and allowed the cross-correlation of force and conductance.[26,27] This newly emerging analysis offers the possibility to connect force plateaus with conductance plateaus measured in unison, and has discerned miniature yet significant relations between force and conductance hidden in the data.[26] Therefore, it is expected that a force-conductance two-dimensional cross-correlation histogram (FC-2DCCH) could unravel the hidden yet important subtleties in the sawtooth modulated data and further extend our knowledge of the role of contact interface in a molecular junction.

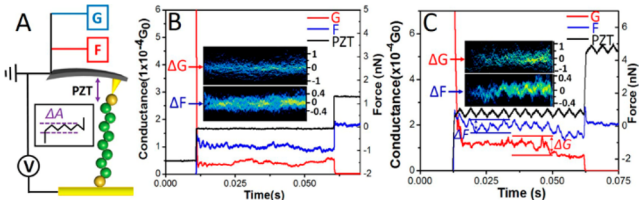

Figure 1. (A) Schematic of the modified conducting atomic force microscopy break junction technique and the sawtooth mechanical modulation signal (black box). In the C8DT molecule, carbon atoms and thiol groups are shown in dark green and dark yellow spheres, respectively. Examples of individual traces without modulation (B) and under modulation ΔA = 0.8 Å (C). The inset in B shows the overlay of 67 non-modulated conductance and force traces. The inset in C shows the overlay of 60 modulated conductance and force traces. The units of the insets in B and C are $1\times10^{-4}G_0$ for conductance and 1 nN for force.

Here we measure the conductance and force of Au-C8DT-Au junctions under sawtooth modulations (Figure 1A) and demonstrate FC-2DCCHs for the modulated single-molecule plateaus. Three modulation amplitudes (ΔA = 0.8, 1.0, and 1.2

Received: October 19, 2014
Published: November 25, 2014

   dx.doi.org/10.1021/ja510738y | J. Am. Chem. Soc. 2014, 136, 17406−17409

Å) are tested, and the data set collected under no modulation is also studied for comparison. The resulting FC-2DCCHs show strongly correlated regions of force and conductance for all three modulation amplitudes, which sharply contrasts with non-modulated data. The evolution of FC-2DCCHs with increasing modulation amplitude for the first time distinguishes the subtle intermediate states of contact configurations. This work adds another dimension to the conventional statistical methods and provides critical hints for further theoretical simulations.

We use the modified conducting atomic force microscopy break junction (CAFMBJ) technique to measure the force and conductance in parallel (see Supporting Information (SI) for experimental details).[28] This technique involves a periodic free-holding process while the AFM tip is retracted away from the substrate.[28] The free-holding process stabilizes a junction and greatly minimizes its dynamic movement. In our study, the free-holding is set to occur after every retraction of 1 nm. With the lifetime of the junction extended by the free-holding, proper mechanical modulations can be carried out without hurting the integrity of a junction.[22] As shown in Figure 1A, the sawtooth modulation manipulates the tip/substrate separation by cycling an elongation followed by a compression at a frequency of 240 Hz, while the junction is free-held. This ensures that the changes in conductance and force are predominantly caused by the mechanical modulation instead of the dynamic fluctuation of the junction. The modulation manipulates the softest part of the junction. In our system, C8DT molecules can be regarded as a rigid body since the C-C bond is much stronger than the S-Au and Au-Au bonds at the contacts.[14,29] Thus, the softest part in our system is the molecule/electrode contacts, which should be the source of most changes induced by the modulations. Typical non-modulated and modulated traces are shown in Figure 1B,C. We see that the force and conductance traces without modulation reveal no obvious feature other than slight variations attributed to the thermo vibration of the junctions.[29] Traces measured under a modulation show regular force fluctuation in accordance with the PZT signal and conductance fluctuations in opposite phase to the PZT signal. This phenomenon is consistent with a previous report,[22] and it is easy to understand that conductance decreases during the increase of PZT signal from the valley to the peak, which extends the junction distance and lowers the efficiency of electron transport.[30] We also notice that modulation does not necessarily induce a conductance change.

We first analyze the data sets by plotting conductance (force) 1D and conductance (force) vs time 2D histograms. Simultaneously measured conductance and force traces with significant features are selected for the data analysis (see SI, section S4 for trace selection method). The conductance 1D histogram for the non-modulated data shows two pronounced peaks at around $2.5\times10^{-4}G_0$ and $0.5\times10^{-4}G_0$ which coincide with the two major bands (blue arrows) in the conductance vs time 2D plot (Figure S1A). These two conductance values match well with previously reported high and medium conductance sets for Au-C8DT-Au junction.[11,12] We ascribe those single-molecule conductance values lower than these two but previously reported to be less populated in our data. The force 1D histogram reveals a dominant peak at around 1.5nN, which matches the rupture force of the junction via Au-Au breaking (Figure S2A).[6,23,31] The successful determination of different conductance sets and the junction rupture force rationalizes our trace selecting method. Under modulation ΔA= 0.8 Å, both conductance (force) 1D and 2D histograms reveal no distinguishable detail (Figure S1B and S2B). This indicates that the1D and 2D histograms wash out the significant features in the modulated data and fail to zoom into the miniatures.

As the SMBJ system was initially built to study single-molecule properties, data analysis approaches to interpret the most repeated features and statistically significant information measured while a single molecule is sandwiched between the electrodes are necessary. To downscale the analysis to single-molecule level, we clip the traces to single-molecule plateaus by excluding those conductance traces without a plateau within the single-molecule conductance range (see SI, section S3 for data clipping method). We then focus on the fluctuation signals (ΔG and ΔF) induced by the mechanical modulations on these single-molecule plateaus. Each single-molecule plateau is offset to zero by subtracting the average value of the plateau, and correlation analysis using many such plateaus could reveal statistically significant information downscaled to the single-molecule level (see the insets of Figure 1B,C).

We present the two-dimensional autocorrelation histogram (2DACH) analysis for force (F) and conductance (C) to explore the relation between two ΔG's or ΔF's (see SI, section S2 for autocorrelation calculation algorithm). By interpreting a single trace in terms of bins, 2DACH essentially describes the correlation degree of data points taken at every bin location. Bin sizes are $2\times10^{-6}G_0$ for conductance and 0.01 nN for force. The correlation degree ranges from −1 to 1 and is plotted in color code (Figure 2). We observe strongly correlated regions

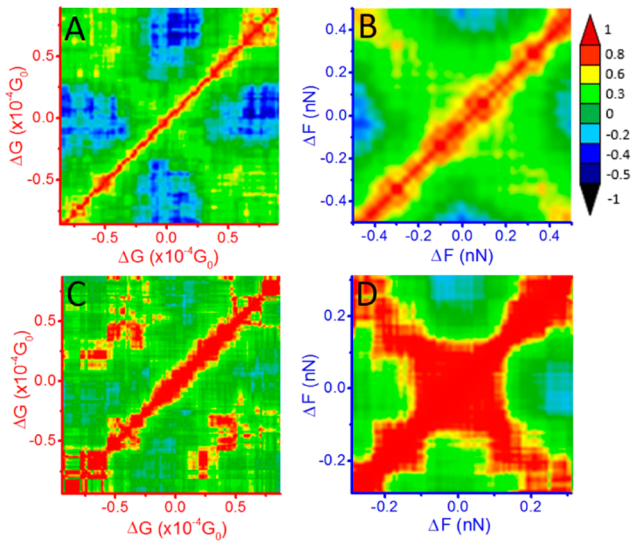

Figure 2. Two-dimensional autocorrelation histogram (2DACH) for non-modulated data (67 traces) and modulated data (ΔA = 1.2 Å, 69 traces). A and B show the C- and F-2DACH for non-modulated plateaus, respectively. C and D show the C- and F-2DACH for modulated plateaus (ΔA = 1.2 Å), respectively. The color bar is the same for all the panels.

distributed along the diagonal line (from bottom left to top right) in each panel of Figure 2. This diagonal line reflects the degree to which a signal correlates to itself, which is supposed to be 1.[23,24] Under no modulation, both C- and F-2DACH show four anti-correlated regions (blue regions), which indicate a rather low possibility of two ΔG's or ΔF's appearing together on the plateaus. These regions relate to where $\Delta G = 0G_0$ correlates with the $\Delta G \approx \pm0.3\times10^{-4}G_0$, and where $\Delta F = 0G_0$ anti-correlates with $\Delta F \approx \pm0.35$ nN, and spread far and wide away from the

dx.doi.org/10.1021/ja510738y | J. Am. Chem. Soc. 2014, 136, 17406−17409

center. We attribute this phenomenon to the few data points beyond $\Delta G = \pm 0.3\times10^{-4}G_0$ and ΔF of ±0.35 nN. Overall, 2DACHs reveal no obvious strong correlated region for non-modulated plateaus. In contrast, under the modulation of ΔA = 1.2 Å, noticeable features in the C-2DACH are the strong correlated regions (red) locating at $(0.48\times10^{-4}G_0, -0.49\times10^{-4}G_0)$. This specifies that the increase in conductance by $0.48\times10^{-4}G_0$ usually emerged with a concurrent conductance decrease by $0.49\times10^{-4}G_0$. It is possible that these two values correspond to two different contact configurations, which frequently took place on the same plateau. Given this effect, we believe the possible change in contact configuration is predominantly induced by the mechanical modulations. Interestingly, the F-2DACH for modulated data shows another strong correlated diagonal line. Similar phenomena are seen for other modulation amplitudes as well (see Figure S3). This newly emerged diagonal line suggests a linear relation that a certain amount of increase in force usually correlated with a force decrease by the same amount on the identical plateau. Since the selected force traces always show linear and regular sawtooth patterns, the average behavior of many such force traces should illustrate a similar degree of increase and decrease at a plateau, and the increase and decrease always correlate with each other. Thus, it is reasonable that F-2DACH produces another diagonal line. This autocorrelation analysis of the modulated data has revealed new details never observed before. Unfortunately, it still fails to bridge the force change with conductance change induced by the mechanical modulations.

The core interest of this study lies in the relationship between a ΔG and a ΔF caused by the introduction of mechanical modulations. FC-2DCCH analysis serves as a powerful tool to achieve this goal by calculating the correlation degree between a force signal and the corresponding conductance signal (see section S2 for cross-correlation calculation algorithm). The same sample traces and bin sizes adopted in 2DACH are also used for FC-2DCCH. We plot the FC-2DCCHs for all data sets in Figure 3. For non-modulated plateaus, the FC-2DCCH shows neither strong nor anti-correlation areas, but some weakly correlated regions dispersed around the center within a range of $\pm0.25\times10^{-4}G_0$ in conductance and ±0.3 nN in force (yellow in Figure 3A). These fluctuations in conductance and force match well with the fluctuations reported in previous measurements.[22] Noting that the junction was free-held while being measured, this fluctuation is not caused by the change of junction separation but by the thermo vibration of the molecule or possible relaxation of the Au-S binding site at a constant junction distance of 1 nm.[22,32] Simulations have suggested that thermo motion of a junction can cause the significant conductance change.[18,29,33]

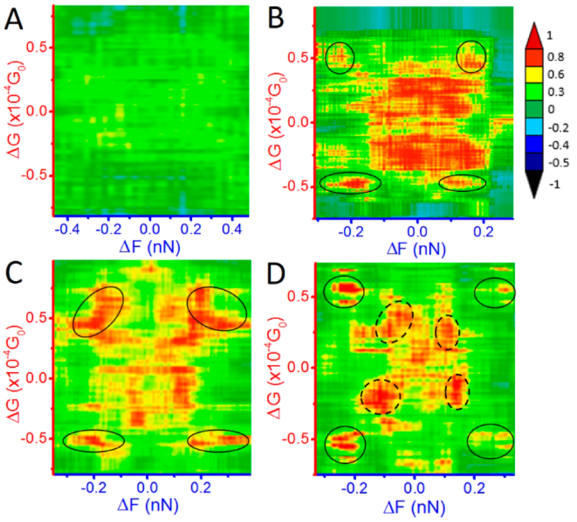

Figure 3. Force−conductance two-dimensional cross-correlation histogram (FC-2DCCH) for non-modulated data (A, 67 traces) and modulated data (B, ΔA = 0.8 Å, 60 traces; C, ΔA = 1.0 Å, 76 traces; D, ΔA = 1.2 Å, 69 traces).

However, FC-2DCCH plots show dramatic changes for the modulated plateaus. Multiple strongly correlated regions (red) can be seen. Interestingly, four specific regions (solid circles) appear consistently for all modulation amplitudes. At modulation ΔA = 0.8 Å, the four regions locate at $\sim(\pm0.48\times10^{-4}G_0, \pm0.18$ nN). They slightly increase to $\sim(\pm0.55\times10^{-4}G_0, \pm0.26$ nN) as the modulation amplitude rises to 1.2 Å. The slight change in conductance with increasing modulation amplitude is consistent with a previous report, which suggested that the increase of modulation amplitude from 0.8 to 1.2 Å would not change the conductance much.[21] Thus, we believe the increase of ΔA from 0.8 to 1.2 Å has little impact on relevant contact configurations but linearly increases the force. The conductance values of these four regions also coincide with those observed in C-2DACH (Figure 2C). Counterintuitively, a positive force at ∼0.2 nN strongly correlates with both positive and negative conductance. The reason is similar to that for the second diagonal line in Figure 2D. A positive ΔF caused by the elongation of the junction induces a conductance decrease, namely a negative ΔG in a FC-2DCCH. However, on the identical plateau, the sawtooth pattern force signal could always occur with both a conductance increase and decrease. A positive force may correlate with any signals, including conductance increase and decrease, that most often occurred with it. Therefore, these correlated regions should distribute in a centrosymmetric manner, as the FC-2DCCHs show. So, the key lies in the net amplitude of ΔG and ΔF instead of their signs. Another interesting feature is that the strong correlated spots related with negative ΔF's usually have a higher intensity than those correlating to positive ΔF's, indicating a stronger correlation between force and conductance when the junction is "compressed". It is necessary to note that the compression effect mainly comes from the molecular angle changes caused by system drifts and contact Au atom motion.[34] We suggest the changes from $\sim0.5\times10^{-4}G_0$ to $-0.5\times10^{-4}G_0$ in conductance and from −0.2 to 0.2 nN in force are related to the switch between two junction conformations which could differentiate in Au-S bonding site, junction length, or molecular angle. Given the little conductance change with increasing modulation amplitude, we believe this switch is independent of modulation amplitudes used in our experiments. Au-S bonding configuration has been reported to be able to alternate among different configurations with the length change of the molecular junction.[12,15,17] A simulation study[18] highly resembling our system illustrated a possible Au-S contact configuration change with a molecular angle tilt (see Figure S5). We believe that this force-induced change in conductance could be due to the change in the coupling energy between thiol and Au. Such coupling energy change will induce a small change in the conductance value, as shown in the 2DCCHs. However, if a large coupling energy change is induced by a large enough force, the transition from one configuration to another configuration could occur.

Noticeable strongly correlated regions distributed around the center show obvious shape changes, from scattered blurred area for ΔA = 0.8 Å to distinct spots for ΔA = 1.2 Å. It has to be noted

dx.doi.org/10.1021/ja510738y | J. Am. Chem. Soc. 2014, 136, 17406−17409

that the scattered center correlation areas for the modulated data are mainly caused by the mechanical modulation, which contrasts with the weak correlated areas also spreading around the center in the non-modulated case. The discrete regions (dashed circles in Figure 3D) correspond to a smaller force and conductance change than the solid circled regions. We suggest that these discrete regions are related to intermediate states through which the junction evolves. In Figure 4, a careful check of detailed

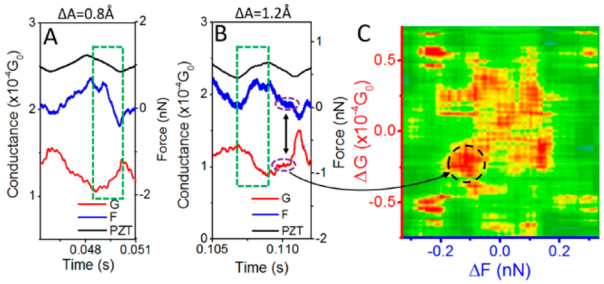

Figure 4. (A,B) Representative zoom-in signal (green dashed square) for ΔA = 0.8 and 1.2 Å, respectively. (C) FC-2DCCH for ΔA = 1.2 Å. In B, the purple dashed circles represent the intermediate force and conductance plateaus which could form the region in the black dashed circle in C.

features in individual plateaus under ΔA = 0.8 and 1.2 Å reverls an exponential increase (decrease) in conductance with the decrease (increase) of junction separation, suggesting a change in tunneling barrier length (see section S6). Given there is no increase in the number of carbon unit of the molecule, this change is essentially contributed by the extra barrier originating from contact interfaces. More importantly, under ΔA = 1.2 Å, we see minor plateaus of both force and conductance (purple dashed circles), which generate strongly correlated regions in FC-2DCCH. This effect occurs for ΔA = 1.2 Å more often, which confirms the existence of the intermediate states and also implies they are more stabilized under ΔA = 1.2 Å. It is noteworthy that some strongly correlated regions that deviated from the regions discussed above are not clear to us yet, and further investigation is needed.

In conclusion, we have measured the force and conductance of Au-C8DT-Au junction using the modified CAFMBJ under sawtooth modulations, and FC-2DCCHs for single-molecule plateaus were demonstrated. The FC-2DCCHs yielded intriguing features: specific changes in conductance closely correlated with force changes induced by the contact configuration switch. Intermediate stabilized junction states during the switch were also discerned. These features were hidden in the data when analyzed by conventional 1D and 2D histogram methods. This work thus for the first time maps the relation between conductance and force involved in a contact configuration transition. We believe that refined experimental controls along with the multivariate data analysis approach can bring us more latent yet significant details in single-molecule junctions.

■ ASSOCIATED CONTENT

Supporting Information

Experimental details, data clipping methods, force histograms, correlation calculation methods, FC-2DCCHs for ΔA = 0.8 and 1.0 Å, exponential fit for conductance, and reprinted junction schematics. This material is available free of charge via the Internet at http://pubs.acs.org.

■ AUTHOR INFORMATION

Corresponding Author

bxu@engr.uga.edu

Notes

The authors declare no competing financial interest.

■ ACKNOWLEDGMENTS

The authors thank the U.S. National Science Foundation for funding this work (Grant Nos. ECCS 0823849 and ECCS1231967).

■ REFERENCES

(1) Kiguchi, M.; Kaneko, S. *Phys. Chem. Chem. Phys.* **2013**, *15*, 2253.
(2) Tao, N. J. *Nat. Nanotechnol.* **2006**, *1*, 173.
(3) Aradhya, S. V.; Venkataraman, L. *Nat. Nanotechnol.* **2013**, *8*, 399.
(4) Jia, C.; Guo, X. *Chem. Soc. Rev.* **2013**, *42*, 5642.
(5) Nichols, R. J.; Haiss, W.; Higgins, S. J.; Leary, E.; Martin, S.; Bethell, D. *Phys. Chem. Chem. Phys.* **2010**, *12*, 2801.
(6) Xu, B.; Tao, N. *Science* **2003**, *301*, 1221.
(7) Venkataraman, L.; Klare, J. E.; Nuckolls, C.; Hybertsen, M. S.; Steigerwald, M. L. *Nature* **2006**, *442*, 904.
(8) Quek, S. Y.; Kamenetska, M.; Steigerwald, M. L.; Choi, H. J.; Louie, S. G.; Hybertsen, M. S.; Neaton, J. B.; Venkataraman, L. *Nat. Nanotechnol.* **2009**, *4*, 230.
(9) Xiang, D.; Jeong, H.; Lee, T.; Mayer, D. *Adv. Mater.* **2013**, *25*, 4845.
(10) Ratner, M. *Nat. Nano.* **2013**, *8*, 378.
(11) Li, X.; He, J.; Hihath, J.; Xu, B.; Lindsay, S. M.; Tao, N. *J. Am. Chem. Soc.* **2006**, *128*, 2135.
(12) Li, C.; Pobelov, I.; Wandlowski, T.; Bagrets, A.; Arnold, A.; Evers, F. *J. Am. Chem. Soc.* **2008**, *130*, 318.
(13) Haiss, W.; Martín, S.; Leary, E.; Zalinge, H. v.; Higgins, S. J.; Bouffier, L.; Nichols, R. J. *J. Phys. Chem. C* **2009**, *113*, 5823.
(14) Arroyo, C. R.; Leary, E.; Castellanos-Gómez, A.; Rubio-Bollinger, G.; González, M. T.; Agraït, N. *J. Am. Chem. Soc.* **2011**, *133*, 14313.
(15) Kaun, C.-C.; Seideman, T. *Phys. Rev. B* **2008**, *77*, 033414.
(16) Dhungana, K. B.; Mandal, S.; Pati, R. *J. Phys. Chem. C* **2012**, *116*, 17268.
(17) Tachibana, M.; Yoshizawa, K.; Ogawa, A.; Fujimoto, H.; Hoffmann, R. *J. Phys. Chem. B* **2002**, *106*, 12727.
(18) Paulsson, M.; Krag, C.; Frederiksen, T.; Brandbyge, M. *Nano Lett.* **2008**, *9*, 117.
(19) Guo, S.; Hihath, J.; Diez-Perez, I.; Tao, N. *J. Am. Chem. Soc.* **2011**, *133*, 19189.
(20) French, W. R.; Iacovella, C. R.; Rungger, I.; Souza, A. M.; Sanvito, S.; Cummings, P. T. *J. Phys. Chem. Lett.* **2013**, *4*, 887.
(21) Xu, B. *Small* **2007**, *3*, 2061.
(22) Zhou, J.; Chen, G.; Xu, B. *J. Phys. Chem. C* **2010**, *114*, 8587.
(23) Halbritter, A.; Makk, P.; Mackowiak, S.; Csonka, S.; Wawrzyniak, M.; Martinek, J. *Phys. Rev. Lett.* **2010**, *105*, 266805.
(24) Makk, P.; Tomaszewski, D.; Martinek, J.; Balogh, Z.; Csonka, S.; Wawrzyniak, M.; Frei, M.; Venkataraman, L.; Halbritter, A. *ACS Nano* **2012**, *6*, 3411.
(25) Wawrzyniak, M.; Martinek, J.; Susla, B.; Ilnicki, G. *Acta. Phys. Pol. A* **2009**, *115*, 384.
(26) Hamill, J. M.; Wang, K.; Xu, B. *Nanoscale* **2014**, *6*, 5657.
(27) Frei, M.; Aradhya, S. V.; Hybertsen, M. S.; Venkataraman, L. *J. Am. Chem. Soc.* **2012**, *134*, 4003.
(28) Zhou, J.; Chen, F.; Xu, B. *J. Am. Chem. Soc.* **2009**, *131*, 10439.
(29) Michael, G.; Mark, A. R.; Abraham, N. *J. Phys.: Condens. Matter* **2007**, *19*, 103201.
(30) Cuevas, J. C.; Scheer, E. *Molecular Electronics: An Introduction to Theory and Experiment*: World Scientific: Singapore, 2010.
(31) Xu, B.; Xiao, X.; Tao, N. *J. Am. Chem. Soc.* **2003**, *125*, 16164.
(32) Demir, F.; Kirczenow, G. *J. Chem. Phys.* **2012**, *136*, 014703.
(33) Hihath, J.; Bruot, C.; Tao, N. *ACS Nano* **2010**, *4*, 3823.
(34) Diez-Perez, I.; Hihath, J.; Hines, T.; Wang, Z.-S.; Zhou, G.; Mullen, K.; Tao, N. *Nat. Nanotechnol.* **2011**, *6*, 226.